Nuclease resistant circular DNAs copurify with infectivity in scrapie and CJD

Laura Manuelidis

Abstract In transmissible encephalopathies (TSEs), it is commonly believed that the host prion protein transforms itself into an infectious form that encodes the many distinct TSE agent strains without any nucleic acid. Using a Φ29 polymerase and chromatography strategy, highly infectious culture and brain preparations of three different geographic TSE agents all contained novel circular DNAs. Two circular "Sphinx" sequences, of 1.8 and 2.4 kb, copurified with infectious particles in sucrose gradients and, as many protected viruses, resisted nuclease digestion. Each contained a replicase ORF related to microviridae that infect commensal Acinetobacter. Infectious gradient fractions also contained nuclease-resistant 16 kb mitochondrial DNAs and analysis of >4,000 nt demonstrated a 100% identity with their species-specific sequences. This confirmed the fidelity of the newly identified sequences detailed here. Conserved replicase regions within the two Sphinx DNAs were ultimately detected by PCR in cytoplasmic preparations from normal cells and brain but were 2,500-fold less than in parallel-infected samples. No trace of the two Sphinx replicases was found in enzymes, detergents, or other preparative materials using exhaustive PCR cycles. The Sphinx sequences uncovered here could have a role in TSE infections despite their apparently symbiotic, low-level persistence in normal cells and tissues. These, as well as other cryptic circular DNAs, may cause or contribute to neurodegeneration and infection-associated tumor transformation. The current results also raise the intriguing possibility that mammals may incorporate more of the prokaryotic world in their cytoplasm than previously recognized.

Keywords Prion · Phi 29 polymerase · Acinetobacter plamids · Neurodegeneration · Cancer · Circovirus

Introduction

Transmissible spongiform encephalopathies (TSEs) such as Creutzfeldt–Jakob Disease (CJD) and kuru of humans, scrapie of sheep, and BSE of cows are caused by a group of related, but incompletely characterized infectious agents. These agents display many fundamental biological and physical properties of viruses. In the spectrum of viruses, TSE agents could represent a link between symbiotic viruses, including commensal viruses that rarely cause disease, and the classical pathogenic viruses that elicit acute host lymphocytic responses and neutralizing antibodies. TSE agents can persist without causing neurodegenerative disease for as long as 30 years, as shown by iatrogenic transmissions of CJD from contaminated growth hormone.

It is increasingly apparent that a long TSE latency in peripheral lymphatic tissues such as spleen (Manuelidis 2003) is not an unusual viral attribute. We harbor many borderline pathogenic agents, and some covert viruses acquire mammalian nucleotide sequences that help them to evade host recognition and defense mechanisms. Others have evolved to subserve unrelated host cell functions, such as retroviral sequences that become part of the chromosomal organization of specific gene classes (Manuelidis and Ward 1984; Taruscio and Manuelidis 1991). Still others can coexist silently within the host. For example, a resident innocuous virus such as the JC papovavirus, commonly carried in the brain (Elsner and Dörries 1992), may cause

L. Manuelidis (✉)
Yale University Medical School,
333 Cedar Street,
New Haven, CT 06510, USA
e-mail: laura.manuelidis@yale.edu

damage only under stressful conditions including infection with another virus (e.g., HIV), or chemotherapeutic immunosuppression. Other resident viruses may be brought out by aging itself (Manuelidis 1994). Such viruses typically originate in the environment.

An environmental origin of TSE agents is strongly implicated by the geographic prevalence and origin of particular TSE agents (Manuelidis 2010; Manuelidis et al. 2009a; Manuelidis et al. 2009b) as well as by their transmission through the gastrointestinal tract and blood (Manuelidis 1994; Manuelidis 2003; Shlomchik et al. 2001). Several unique strains are geographically restricted, such as CJD isolates from Japan, the kuru agent from New Guinea, and the recent epidemic BSE agent that originated in the UK (Manuelidis et al. 2009a; Manuelidis et al. 2009b). Transmissions of these three geographic CJD agents to normal wild type (wt) mice, and to monotypic neural cells, demonstrate that each of these agents induces its own distinct incubation time and neuropathologic profile. Additionally, all three are different from endemic sheep scrapie and human sporadic CJD (sCJD) agents (Manuelidis et al. 2009a; Nishida et al. 2005). The epidemic outbreak of BSE, and its dramatic reduction after removal of the environmental source, further emphasizes a pathogen that is not spontaneously generated by the host. Kuru also disappeared after cannibalism ceased and has not reappeared for >30 years. Therefore, one might reasonably expect to find foreign nucleic acids derived from the environment in TSEs, possibly in a cryptic or latent form.

Purification and filtration studies show TSE infectious particles are larger than plant RNA viroids (~350 nt) and smaller than hepatitis B, a circular DNA virus that replicates via reverse transcriptase (~45 nm, ~160S). Infectious TSE particles are >20 nm by membrane filtration, and have a homogeneous viral size by field flow fractionation and HPLC (of 90–120S and $\sim 3 \times 10^6$ Da, respectively), with a viral density of 1.28 g/cc. These features indicate a protein–nucleic acid complex rather than a pure protein (Manuelidis 2003; Sklaviadis et al. 1992). Virus-like particles of 25 nm are observed in infectious subcellular preparations, in cytoplasmic arrays of infected brains and in cultured cells with high infectivity (Manuelidis et al. 2007). These particles are resistant to nuclease digestion, a characteristic of viral genomes protected by nucleic acid binding protein(s). Treatments that disrupt viral–nucleic acid complexes, such as GdnSCN and boiling in SDS, decrease TSE infectivity by ~3 logs (Manuelidis et al. 1995). They also disrupt the RNA and 60 kDa protective capsid of a copurifying endogenous retrovirus (Akowitz et al. 1994; Manuelidis et al. 1995). Although retroviruses are not the TSE infectious agent, their association with infectivity can have functional consequences.

A murine retrovirus enhances exosomal release of TSE agent (Alais et al. 2008), and an HIV gag precursor protein is required for permanent infection of cells by a cervid TSE agent (Bian et al. 2010).

Copurification studies raised the possibility that a retroviral binding protein might encapsidate a TSE agent nucleic acid (Akowitz et al. 1994; Manuelidis 1997). Normal cell proteins might also function to protect a "small TSE virino genome", as hypothesized by Dickinson to account for the many different scrapie strains, as well as their infrequent and limited mutation (Bruce and Dickinson 1987). Because normal host prion protein (PrP) aggregates as amyloid and resists limited proteolysis (PrP-res) after infection (Diringer et al. 1983; Merz et al. 1983; Prusiner 1982), Dickinson later assumed that PrP protected a TSE genome. Indeed, PrP selectively binds RNA molecules of 1–2.5 kb and protects RNA from nuclease digestion (Geoghegan et al. 2007). However, ultrastructural antibody and purification studies demonstrate that TSE-specific virus-like particles lack PrP (Manuelidis et al. 2007). Thus, it is more likely that the infectious particle uses host membrane PrP as its required cell receptor, and during this interaction, induces misfolded PrP-res (Manuelidis 1997; Manuelidis et al. 2007). This PrP receptor concept explains the resistance of PrP knockout mice to TSE infection and is also consistent with host PrP mutations that alter susceptibility to infection, as well as induction experiments showing high PrP is involved in the elaboration of nanotubes and cell-to-cell contacts used for viral transfer (Miyazawa et al. 2010). Moreover, the late appearance of PrP-res in animal infections, its separation from infectivity, and the activation of early host responses to the agent (Manuelidis 2003; Manuelidis 2007; Sun et al. 2008) all favor this parsimonious viral model.

Host PrP is clearly involved in susceptibility and pathogenesis, but the prion hypothesis posits that misfolded PrP-res itself, without any nucleic acid, is the infectious agent. This concept revives the self-catalytic infectious protein model of tobacco mosaic virus (TMV). The TMV infectious protein concept, awarded a Nobel Prize, ignored the nucleic acid that was present in infectious preparations. Ultimately, Rosalind Franklin correctly modeled the infectious RNA inside the TMV protein shell (Franklin 1956). Although the coding capacity of nucleic acids was obvious by 1982, and scrapie preparations contained >10 μg/ml of nucleic acid, the prion hypothesis cited its similarity to the incorrect TMV concept as precedent (Prusiner 1982). Because PrP was later found at high levels in normal cells, PrP-res became the infectious form of host PrP. The term PrP scrapie (PrP^{sc}) or $PrP^{species}$ (e.g., PrP^{mo}) was also used to designate all the different human and animal TSE agents (Prusiner et al. 1995), a classification that obscured the

fundamentally distinct strains that are independent of species PrP. This prion concept was also incompatible with the same PrP-res pattern of different strains in the constant wt mouse brain (Manuelidis et al. 2009a; Manuelidis et al. 2009b; Nishida et al. 2005). Other tests to show that PrP-res encodes specific strains present additional complications for the prion hypothesis. For example, different PrP-res patterns in various tissues and cell types does not alter the agent characteristics. The agent, but not the host PrP-res pattern, breeds true (Arjona et al. 2004; Manuelidis et al. 2009a). Mutations of the PrP gene also do not determine the strain, e.g., the identical human 102L PrP mutation yields vastly different CJD agents in Japan and the USA, further implicating geographically defined environmental infections.

PrP is claimed to "mutate" itself (by some unknown mechanism), to spontaneously generate infectivity, and to "evolve" without any nucleic acid (Li et al. 2010; Edgeworth et al. 2010). However, claims of no nucleic acids of >50 nt in infectious preparations rest on limited data only from Prusiner's prion group (Safar et al. 2005). In contrast, modern molecular tracing methods such as radioactive labeling, RT-PCR, and cloning methods have yielded RNAs as large as 5,000 nt in nuclease digested TSE preparations (Akowitz et al. 1994; Manuelidis 2003). Moreover, both the Marsh and Weissmann groups independently uncovered nucleic acids of >300 nt in Prusiner's purified prion protein preparations (Aiken et al. 1989; Oesch et al. 1988), and subsequent samples have not been obtainable for independent analysis. Thus, common statements that the TSE agent is an infectious protein without nucleic acid (e.g., Bian et al. 2010; Falsig et al. 2008; Li et al. 2010; Nicoll and Collinge 2009; Zou and Gambetti 2007) ignore positive evidence of nucleic acids in infectious preparations. Moreover, recombinant PrP-res made in vitro, without added brain or other components such as nucleic acids and lipids, has not shown reproducible infectivity, and when brain and related components were added, only low infectivity of agents remarkably similar to laboratory strains were produced (Couzin-Frankel 2010; Manuelidis 2007; Supattapone 2010). Conversely, myeloid cells with minute amounts of PrP, and no detectable PrP-res, contain very high infectious titers (Baker et al. 2002).

The empirical size of the TSE infectious particle is sufficient to encompass a nucleic acid genome of 1–4 kb (Manuelidis 2007). This size range includes hepatitis δ, a satellite virus with a genome of 1,682 nt (Ma et al. 2003), circoviruses found in both plants and animals (16–22 nm, ~2,500 nt), and circovirus-like Anneloviruses of primates. The latter are commensal and, like TSE agents, can also persist in myeloid cells. Some circoviruses even contaminate commercial vaccines (Davidson and Shulman 2008; Vincent et al. 2005; Kekarainen et al. 2009)), a potential source of common

infection. Unlike TSE agents, porcine circovirus 2 elicits an inflammatory tissue response. Nevertheless, the structurally related ubiquitous human Torque tenovirus (TT, an enteric Annelovirus) has other similarities to TSE agents. It is resistant to extreme physical and chemical conditions of heat and pH (Davidson and Shulman 2008) and has been isolated from cerebrospinal fluid of a patient with sub-acute dementia (Maggi et al. 2001). Such features encouraged an investigation of circular DNAs in infectious TSE preparations. Nick translation in 1981 had already indicated that circular mitochondrial DNA copurifed with CJD particles in guinea pigs (Manuelidis and Manuelidis 1981) and >500 bp of mitochondrial DNA were subsequently identified in Prusiner's purified hamster scrapie preparations (Aiken et al. 1990). Because nick translation would not have uncovered single stranded (ss) circular DNAs, a strategy for their detection was developed. Rather than trying to amplify a specific group of circular viruses such as the human TT virus by some possible sequence conservation, a more general approach could be more productive. Circular viral DNAs typically replicate by a rolling circle mechanism, and faithful sequence amplification of pg levels of these DNAs can be achieved with φ29 polymerase (Dean et al. 2001; Mizuta et al. 2003). This strategy should also uncover small new retroid hepatitis B-like DNAs in TSEs (Manuelidis et al. 1988). Finally, a fundamental, though generally unappreciated, biological reason for considering a circular DNA viral genome is based on the frequent transformation of cells grown from TSE-infected brains (Manuelidis et al. 1987). Cells exposed to infectious brain preparations also transform and generate huge solid tumors in nude mice (Manuelidis et al. 1988; Oleszak et al. 1986). Circular viral DNAs often induce tumors (e.g., papillomaviruses) and papovaviruses can cause malignant brain tumors.

This report describes two novel circular plasmid-related DNA sequences of 1.8 and 2.4 kb isolated from high titer N2a-22L scrapie cell gradient fractions (Liu et al. 2008; Sun et al. 2008). These circular DNAs were also identified in brain preparations from 263K scrapie-infected hamsters and from FU-CJD-infected mice. A region of these sequences was also detected in uninfected cells and brain by PCR, albeit at very low levels as compared to infected cells. It is not yet known if the 1.8 and 2.4 kb sequences are involved directly in TSE infection, neurodegeneration, or neoplastic transformation. Nevertheless, the strategy presented here is robust and capable of uncovering additional new classes of circular DNAs in mammalian cells. At the very least, the present experiments underscore substantial and reproducible coding nucleic acids in nuclease-treated TSE preparations. These circular DNAs also raise the possibility that mammalian cells and tissues may incorporate low cytoplasmic copies of previously unsuspected environmental DNAs.

Results

Overall strategy The experimental strategy rests on the ability of the highly processive φ29 polymerase enzyme to preferentially target and faithfully synthesize circular DNA by a rolling circle mechanism. The resultant large DNAs can then be cut by restriction enzymes and specific fragments compared with those in various controls such as water. Since random primers were used, and the temperature optimum for this enzyme is 30°C, some random primers will anneal and form a circular substrate for the enzyme. When heterogeneous RNA that binds random primers is included in the reaction (see "Materials and methods"), no detectable DNA is synthesized. Similarly processive enzymes, such as PCR polymerases, will also make dimers and multimers in control water reactions when the primers have some sequence homology to each other, and/or are done at lower temperatures that allow primer annealing. Thus, when random primers are available, φ29 polymerase water controls will show background DNA synthesis here and in other laboratories (Navidad et al. 2008). In any case, these background DNAs were irrelevant because they did not yield the same restriction enzyme bands as the infectious samples, and none of the Sphinx sequences identified here could be found in the controls by high-cycle PCR (detailed below). To confirm that the circular structures of obtained sequences were not artifactual, circular sequences were additionally enriched by chromatography prior to φ29 polymerase reactions. Finally, to substantiate the reproducibility and prevalence of new DNA sequences that cosediment with infectivity, different cell types, and tissues, as well as distinct agent strains, were evaluated.

N2a cultures infected with 22L scrapie were initially analyzed for the following reasons. First, they produce stable high titers of agent, comparable to those found in brain and can be replenished rapidly. Second, infected cells are much less complex than brain tissue, an advantage for agent purification. Third, they do not show severe neurodegenerative changes that can compromise purification and nucleic acid extraction. Fourth, the level of infectivity in the cell preparations used here were titered by both the rapid tissue culture infectious dose (TCID) assay and also confirmed by standard animal assays (Liu et al. 2008; Sun et al. 2008). This rapid TCID culture assay, unlike the scrapie cell panel assay (Edgeworth et al. 2010), has no false positive background and was also accurate for FU-CJD mouse brain. Titration is essential for assessing the representation of DNA sequences with respect to agent particles, and this rapid assay made it possible to assay numerous sucrose fractions from multiple preparations. Fifth, since TSE agents might be commensal, a TSE-associated sequence might ultimately be found in normal preparations. Therefore, subtractive strategies were not used

(Dron and Manuelidis 1996), and uninfected parallel preparations were compared for the prevalence of new sequences. Sixth, there are typically ~1LD$_{50}$ of agent per 1–10 N2a-22L-infected cells; a TSE-associated ss circular DNA of 2 kb could contain as little as 1–10 pg of this DNA in 10^7 cells. Thus, some type of amplification would be required to identify this DNA on gels by staining. Φ29 polymerase selectively favors synthesis of circular and/or ssDNA over linear dsDNAs and can amplify full-length sequences ≥8,000-fold because it can read >7,000 nt without strand displacement (Dean et al. 2001). The DNA synthesis is also error free. This allows one to directly sequence eluted bands of interest after restriction enzyme digestion. Because the enormously long DNA products contain multiple repeating copies of the circular DNA, the necessity of cloning multiple small fragments, as well as trying to determine the orientation and relationship of diverse non-overlapping sequences, is avoided. Restriction enzyme separation of larger DNAs of interest also allowed ligation of designed sequences for direct sequencing. Seventh, the comparison of animal brains from two different species infected with other TSE agents (263K scrapie-infected hamsters and FU-CJD-infected mice) further clarified the representation as well as the cell and tissue associated origin of the sequences uncovered here.

Demonstration of circular DNA Figure 1 shows a representative example of both the long undigested (>15 kb), and the restriction enzyme digested Φ29 polymerase products. As noted above, water with random primers will always give some background synthesis; Fig. 1a, lane 1 shows a smear of products from water. The replicative circular form of Φ×174 DNA, another control, yielded a more homogeneous long DNA product (lane 2). Nucleic acids from the highly infectious 22L scrapie 65% sucrose gradient sediment (fraction A, lane 3) that contained 85% of the infectivity applied to the gradient, as well as fraction B from the 20% sucrose step with 1/50th the titer of A (lane 4) also yielded very long DNA products. Several 6 nt recognition restriction enzymes were used to linearize these samples. Digestion with Pst I is shown in Fig. 1a. Pst I cuts Φ×174 DNA at only one site, yielding the predicted 5.4 kb band with no residual long DNA (Fig. 1a, +PstI lane 2). Water yielded a smear of many different DNA fragments with Pst I (+PstI lane 1), and these were consistent with complex annealing of primers with the Pst I sequence. Infectious sucrose fractions A and B displayed very different band patterns (+PstI lanes 3 and 4) that were not seen in the water and Φ×174 DNA controls. In the highly infectious A sample, most of the DNA was uncut by Pst I, and minor multimer-like repeat bands between ~1.5 and 2.5 kb were seen only in fraction A (lane 3). This indicated that this infectious fraction contained DNA sequences not present in fraction B, in accord with previously shown protein and PrP
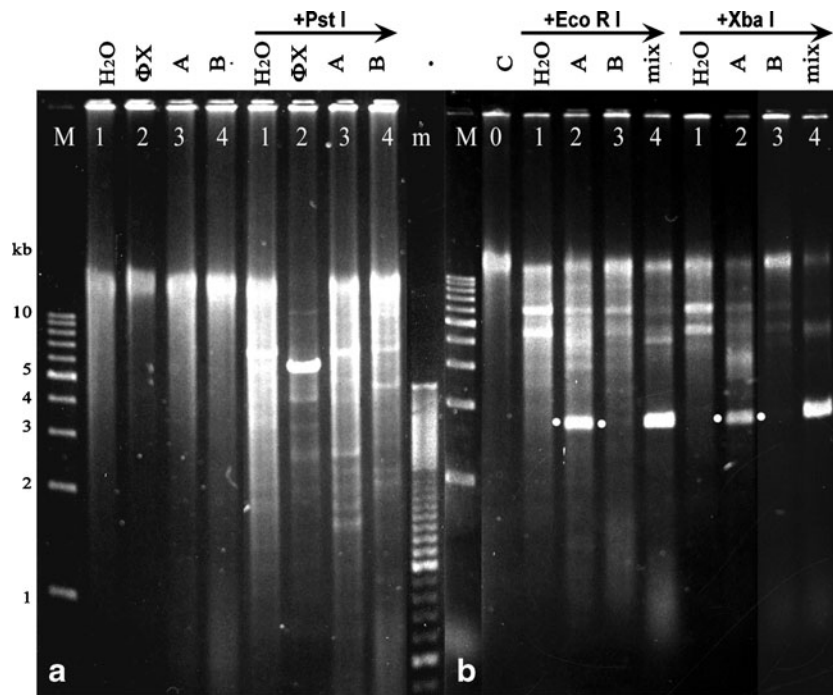
Fig. 1 1% agarose gel with Φ29 polymerase products. Panel **a** Uncut products from the water and Φ×174 controls (*lanes 1* and *2*) and murine N2a-22L scrapie sucrose fractions A and B with high and low infectivity, respectively. The major DNA products migrate at ≥15 kb before restriction enzyme digestion. The various restriction enzymes, as indicated, yield different band patterns in scrapie samples and controls, and only the Φ×174 gives its predicted 5.4 kb Pst I band with no residual uncut material. No DNA was seen in samples with heterogeneous RNA that bound the random primers. Panel **b** Other enzymes and the mix fraction made from infectious material that was purified by a second sucrose gradient after DNAse 1 digestion. The 1.8-kb bands are visible only in the scrapie fractions with high infectivity. Markers *M* are 1–10 kb, as indicated and the 5-kb band contains 9 ng DNA while the other bands contain 3 ng; *m* are 100 bp markers and gel was stained with Sybr gold

differences in these two fractions (Sun et al. 2008). It also showed that most of the synthesized DNA from gradient fractions did not contain a Pst I site since most DNA remained at >15 kb.

Other enzymes revealed more major and unique DNA fragments in the 22L infectious gradient fractions. Figure 1b shows that *Eco*RI and *Xba*I digestions both yielded a major DNA band of ~1.8 kb in the infectious A fraction (dots in lanes 2) but not the B fraction (lanes 3). A mixture of several sucrose gradient steps that contained 10% of the gradient infectivity (from just above the most infectious 65% sucrose step) was also pooled, digested with DNAse I, bath sonicated in sarkosyl, and applied to a second sucrose step gradient prior to nucleic acid extraction (see "Materials and methods"). This was done to test if TSE infectious particles that were resistant to DNAse I would again sediment into 65% sucrose. This fraction, labeled mix in Fig. 1b, also shows the same major *Eco*RI and *Xba*I restriction band of 1.8 kb (lanes 4). Nucleic acids from other infectious 22L scrapie gradient preparations yielded a comparable 1.8 kb band. This band was never seen in numerous water controls.

Because tissue culture cells are exposed to serum and other components such as trypsin, it was important to evaluate infected tissue not exposed to such factors. A hamster brain infected with the 263K scrapie agent that was partially purified by a comparable sucrose step gradient was used for comparison. This preparation also yielded the same ~1.8 kb *Eco*RI band, albeit with more background, as shown in Fig. 2a (lane 1, at dots). Furthermore, *Xba*I digests of this hamster 263K brain preparation also gave the identical band when run in parallel with the 22L preparation (data not shown), indicating the band was likely the same in cultured cells and brain. Digests with *Bgl*II also uncovered a different ~2.4 kDa band, and this was present in both the 22L infectious A and sucrose mix fractions. Figure 2a shows this band in lanes 2, 3, and 5. It is not present in the water sample (lane 4). Because the material from this gradient was limited, it was pertinent to find if one could make more DNA from the initial Φ29 polymerase sample in a second reaction spiked with the first polymerase reaction product. More of this DNA was synthesized, as shown in lane 3, but there was an increase in background and small DNA products as compared to the initial synthesis (lane 5). In sum, there were at least two different bands of interest in these very different TSE models. The 1.8 and 2.4 kb bands were further analyzed, as representatively depicted, and sequenced.
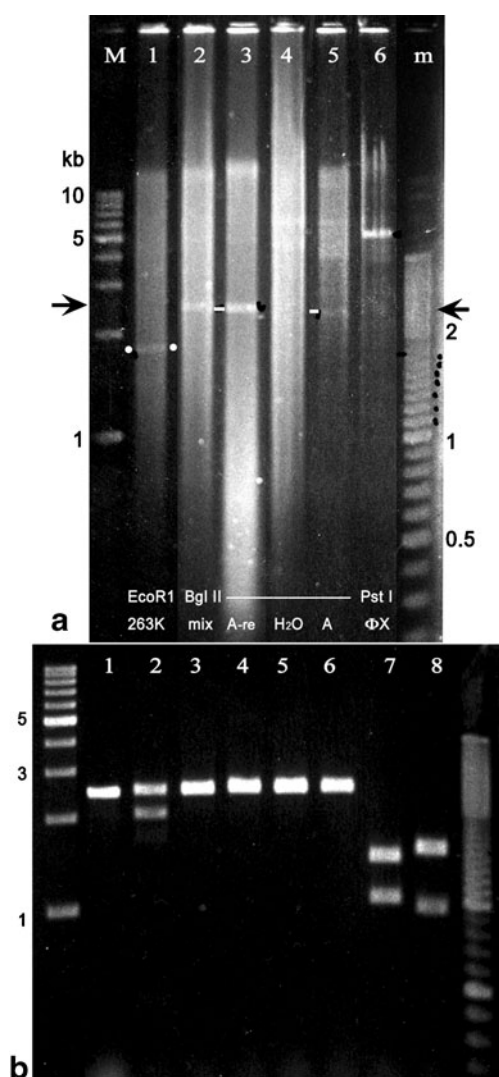
Fig. 2 Agarose gels of Φ29 polymerase products and other restriction digests/samples, as well as purified bands used for sequencing. Panel **a** The 263K scrapie-infected hamster brain has a comparable 1.8 kb band (*lane 1, at dots*) with *Eco*RI digestion. *Bgl*II cuts of mouse N2a-22L scrapie samples show an additional 2.4 kb band (*lanes 2, 3 ,5 at dots* and *lines between arrows*). In *lane 3*, the gradient A fraction was used to make more DNA by a second round of Φ29 polymerase. The 1.8 kb band is re-synthesized, but there is a smear of smaller DNAs in comparison to the initial sample (in *lane 5*, loaded at half the amount of *lane 2*). Panel **b** The 2.4 kb *Bgl*II band after RBgl primed PCR and gel purification (*lane 1*). *Parallel lanes* were cut with different restriction enzymes: *Eco*RI (*lane 2*), *Hin*dIII (*lane 3*), *Kpn*I (*lane 4*), *Xho*I (*lane 5*), *Pvu*II (*lane 6*), *Rsa*I (*lane 7*), and *Hae*III (*lane 8*)

Sequencing of fragments and preferential synthesis of circular DNAs The 2.4 *Bgl*II band was cut from an agarose gel, ligated to the RBgl primer pair and subjected to PCR to amplify the 2.4-kb band. This band was tested with a set of restriction enzymes to find a site that would separate both ends, as shown in Fig. 2b. The two bands after digestion with *Rsa*I were isolated for initial sequencing from each RBgl end. *Eco*RI restriction yielded a minor band of

~2.1 kb (lane 2), and this was also isolated for sequencing. It was completely homologous to murine mitochondrial DNA. A similar strategy was used for the 1.8 kb band that was linearized with *Xba*I. This band was ligated to the 6F4/*Xba* primer pair, amplified by PCR, purified from a preparative gel (Fig. 3a, lane 4), and cut with *Hin*dIII into two end fragments (Fig. 3a, lane 7) to obtain internal sequences for primer walking.

Figure 3 additionally demonstrates products using the chromatography strategy to enrich circular sequences. Chromatography further verified the preferential synthesis of circular ssDNA sequences by Φ29 polymerase. As a control, benzoylated napthoylated DEAE cellulose (BzNp DEAE) spin columns were first evaluated using two sets of linear gel makers (a mixture of the 1 kb "M" and 100 bp "m" ladders) that were mixed with Φ×174 supercoiled RF circles of 5.4 kb. This mixture is shown before chromatography in Fig. 3a, lane 1. The supercoiled circular Φ×174 DNA (at dot) runs faster than the 5 kb ds linear DNA band, as expected. After chromatography, an aliquot of the first eluted fraction that should be enriched in linear dsDNA shows the linear markers are recovered (lane 2). In contrast, the eluted ss and circular fraction shows only the Φ×174 band (lane 3, at dot). The slightly slower migration of this Φ×174 DNA after chromatographic separation is consistent with some nicking of the super-coiled circles during their purification. These elutes of linear ds DNA and ss/circular DNA were then both incubated with Φ29 polymerase to test for the enzyme's preferential synthesis of circular DNAs. Cleavage with *Pst*I verified the circular 5.4 kb-specific Φ×174 DNA only in the circular chromatographic fraction. A smear of DNA, without detectable Φ×174 DNA, is seen in the ds sample (lane 5) and is clearly different than the strong positive synthesis of the Φ×174 band in the circular DNA fraction (lane 6). As expected, this newly synthesized ds linear 5.4 kb Φ×174 DNA now migrates at its ds linear size, i.e., more slowly than the supercoiled and nicked circles. BzNp DEAE was also used on less pure 263K brain preparations and further showed that the 1.8- and 2.4-kb sequences above could be enriched, consistent with their circular structure in the original infectious preparations.

Protected 16 kb mitochondrial DNAs show sequence fidelity BzNp DEAE chromatography of infectious fractions also selectively enriched for circular mitochondrial sequences that were not always apparent in the initial Φ29 polymerase sample digestions. Figure 3b shows prominent new bands in the circular 263K hamster brain chromatography fraction (lanes 1 and 2). These were again completely different than those seen in the water controls. The hamster brain bands also showed a very different pattern than those in the mouse cell preparations (lanes 3, 4, 5, respectively).
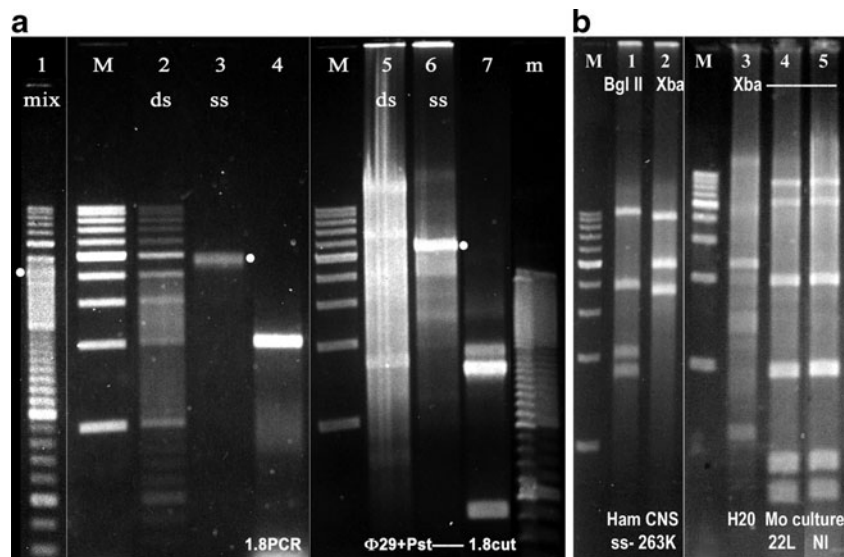
Fig. 3 DNAs from BzNp DEAE chromatography to enrich circular ss DNAs and the preparative 1.8 kb bands used for sequencing. Panel **a** A control of the linear markers *M* and *m* mixed with circular RF Φ×174 plasmid DNA (at *dot*) prior to chromatography (*lane 1*). *Lane 2* shows the post chromatography linear dsDNA fraction, and *lane 3* shows the circular DNA fraction. In this latter fraction, only the circular plasmid band is evident. Both the linear and circular DNA fractions were then subjected to Φ29 polymerase synthesis and cut with Pst 1 to further assess circular DNA. Only the circular chromatography fraction yields the circular plasmid. *Lane 4* shows the 6F4 primer annealed 1.8 kb PCR product and *lane 7* shows the *Hin*dIII fragments used for initial sequencing of Sphinx 1.76 DNA. Panel **b** The pattern of restriction bands in hamster brain after BzNp DEAE selection of ss (mitochondrial) circular DNA (*lanes 1* and *2*). The hamster *Xba*I bands are completely different from those seen in water (*lane 3*). The mouse preparations from both infected N2a-22L and uninfected N2a cells (*lanes 4* and *5*) show the different mouse-specific mitochondrial band pattern

The mouse bands were of the same intensity (quantity) in uninfected (Nl) and infected (22L) cell lanes, as would be expected for mitochondrial sequences. These mouse and hamster species differences further indicated no detectable cross contamination of the hamster preparation that could account for the common 1.8 and 2.4 kb bands. The prominent mitochondrial bands in each of these digestions added up to 16 kb, indicating that Φ29 polymerase synthesized full-length mitochondrial circles. The mouse bands from N2a cells were consistent with murine mitochondrial sequences in the genbank database, except that there was an extra band at ~900 bp in our samples, most likely due to an absence of one *Xba*I site in our cultured mouse cells and/or a difference in different mouse inbred lines used. Although the hamster restriction fragments did not match some predicted bands of the single complete mitochondrial sequence in the database for Syrian hamster (*Mesocricetus auratus*), sequencing of representative bands from samples of each species demonstrated 100% homology to their mitochondrial DNAs in genbank. For example, 1,020 nt starting at 1,672 of the genbank mouse mitochondrial sequence, as well as 1,187 nt starting at position 3998, showed complete nucleotide identity. Hamster examples included 100% identity of 995 nt starting at 5,5770, and 973 nt starting at 10,977 of the complete *M. auratus* mitochondrion sequence. Thus, the circular sequences derived by Φ29 polymerase here were of high fidelity and clearly mitochondrial. Copies of full-length mitochondrial DNA in agent-enriched sucrose fractions clearly survived extensive nuclease digestion, as they were found after exhaustive Benzonase and DNAs I digestions.

Structure and coding regions of 1.8- and 2.4-kb circles Sequencing of the 1.8-kb fragment confirmed it was a circular DNA with structural and coding elements similar to a plasmid replicase (Rep) domain. The circular DNAs identified by this approach are here designated SPHINX sequences, an acronym for **S**low **P**rogressive **H**idden **IN**fections of variable (**X**) latency because they are enriched in infectious TSE preparations. A diagram of Sphinx 1.76 with useful single restriction sites is shown in Fig. 4. Position 1 indicates the *Xba*I site used for initial sequencing, and this site also contains an adjacent *Eco*RI sequence. Thus, both enzymes give the same size band on gels. In 2005, when first sequenced, there were no significant sequence homology by nblast to any nucleotide sequence in the database, including environmental samples. However, translation of a potential open reading frame (detailed below) showed similarity with amino acid (aa) sequences of a replication initiation protein of bacterial plasmids (small circular viruses that infect bacteria and can confer special evolutionary advantages such as antibiotic resistance). For example, the translated protein has 28%
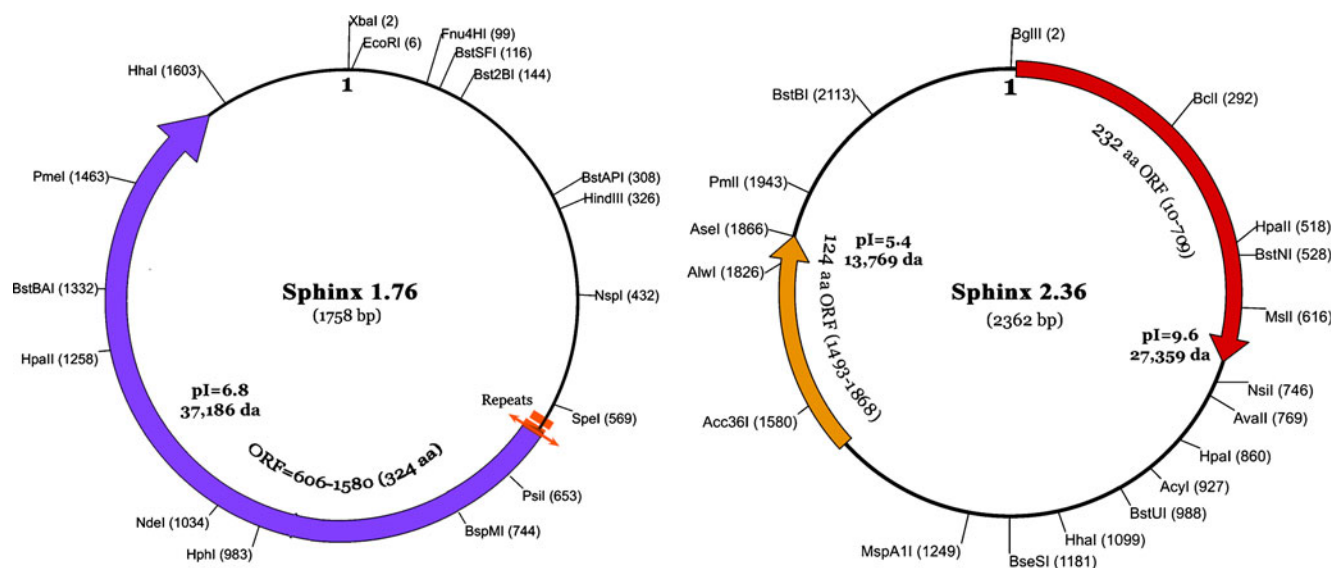
Fig. 4 Maps of Sphinx 1.76 and Sphinx 2.36 with useful single restriction sites and ORFs (*arrows*). The first nucleotide (*1*) indicates where these sequences were cut for annealing primer-ligators. Tandem repeats, consistent with iterons, are present in Sphinx 1.76 as well as a Leucine Zipper motif (see text). These sequences were deposited in genbank and are accessible as HQ444404 and HQ444405

identity of 78/269 aa of accession P17492 ($5e^{-22}$), only a small portion of its full length. This first homology was in the functional plasmid replicase region. For reference, it was significant since 10^{-12} indicates a random possibility of one in a trillion, and lower numbers are even less probable. Because of this initial homology, I suggested several years ago that a TSE agent might code for a replication protein (Manuelidis 2007). Subsequent analyses of the growing database showed Sphinx 1.76 had homology to the Rep 3 superfamily, with 58% aa identity to *Acinetobacter junii* plasmid SH205 and a comparable homology to a plasmid from *Acinetobacter baumannii*. These are the best matches as of this writing and clearly not random, with a chance occurrence of less than 1 in10^{-95}. Nucleotide sequence matches are also now clearly non-random in the replicase ORF of an *A. baumannii* plasmid (676/976 bases) with a probability of $<10^{-105}$. The gaps and mismatched bases seen throughout this alignment are unlikely to be due to sequencing errors generated here, especially given the fidelity of the mitochondrial sequences determined above from the same preparations. Thus the Sphinx 1.76 circular DNA is clearly different from the common bacterial plasmid. Moreover, since the Acinetobacter plasmid with the best match was 12.2 kb (less than the synthesized 16 kb mitochondrial circle), it could be easily synthesized in the reactions here. Sphinx 1.76 was much smaller, further indicating it is likely to be an independent new entity. The sequence of its 324aa coding region is as follows:

M S D L I V K D N A L M N A S Y N L A L V E Q R L
I L L A I I E A R E T G K G I N A N D P L T V H A

GSYINQFNVQRHTAYQALKDACKDLFARQF
SYQEKRERGRINITSRWVSQIGYMDDTATVEI
IFAPAVVPLITRLEEQFTQYDIEQISGLSSAYAV
RMYELLICWRSTGKTPIIELDEFRKRIGVL
DTEYTRTDNLKMQVIELALKQINEHTDIT
ASYEQHKKGRVITGFSFMFKHKKQNSDKTPD
TNASSPRIVKHSQIPTNIVKQPENAKMSDLE
HRASRVTGEIMRNRLSDRFKQGDESAIDMM
KRIQSEIITDAIADQWESKLEEFGVVF*.

Notably, just before this ORF, there are a series of unique repeats (Fig 4 graph) that are consistent with general features of iterons found before replication initiation sites of circoviruses (including plant nanoviruses), primate anneloviruses, and plasmids. The direct repeats here did not match the repeats of the iterons of those viruses, further suggesting the 1.76-kb circle could encode a unique but functional initiator of replication. The first set of shorter tandem repeats (3.7× with minor variation with a 10mer periodicity) is TTTTAA AGT-TTTTAAATGC-TTTTAAATGC-TTTTAGA. The variant bases are underlined, and 43 nt further downstream, there are three copies of the perfect 22 nt tandem repeat GTTTACCGATCAATACCCCTAC. The ORF, interestingly, has a predicted size of 37,285 Da, and hence would be obscured by tissue-specific glycosylated PrPs that migrate as 34–38 kDa proteins on gels. The ORF has a pI of 6.8. Further Prosite analyses showed a leucine zipper motif (aa underlined above). This motif is typically part of DNA binding domains most often found in eukaryotic regulatory proteins.

Sphinx 2.36, diagrammed in Fig. 4, showed less DNA sequence identity to genbank sequences than Sphinx 1.76. Its ends, but not its middle ~2,000 nt have a 9e-45 match with ≤75% identity in terminal regions. Two open reading frames of >120aa were identified. The larger 232aa sequence had 58% identity over 281aa of its length with a putative *A. baumannii* replication plasmid yielding a probability of $<10^{-70}$. It was also homologous to the *Acinetobacter radioresistens* SK82 plasmid sequence, albeit over a shorter aa length. Both homology regions are part of the Rep 1 superfamily involved in rolling circle replication. The larger ORF diagrammed is 27,359 Da, a protein that would also be covered by the deglycosylated form PrP of 27 kDa. Its pI is 9.6 and, like PrP, could be similarly insoluble at physiological pH. The smaller 124aa ORF of 14 kDa has less convincing homology to any protein in the database, (no *e* value of greater probability than 10^{-11}). The larger and smaller Sphinx 2.36 ORFs are respectively:

MQEQYLWTQVDFKVGSETSIKALKAATKLKG
CGQFLLFRNYYTIDQIKLEKFHVCGQHLLCPM
CAGIRAARSMNRYIQRIEEIMRQNRKLKPVLI
TLTVKNGEDLQERFEHLTGSFKTLLQ
RYRDFKKKGRGFNQFCKIDGGFYTTEYTY
NETTQQWHPHIHIFALVTDRIDQEELAETWH
DITLDSYIVDIRRVKKTKEHGYAKAVAEVCK
YALKFSDLSTEKTFQAFFDP

and MNHKLIAIDQELTMKLHNPNP
NEPTNLQMLVAEIKKSASSSYHGGYIQVPFR
VECASYTRLEALVKHTGSSRNKIMNDLL
RIGIETLAASLDDETIKTLFEIETSI
TADLYASGKMKSGDQSDD.

Cytoplasmic preparations are the source of Sphinx DNAs
Even though the Sphinx 1.76 and 2.36 gel bands were not directly visible in Φ29 polymerase synthesized samples that contained little or no infectivity, their distant homology to Acinetobacter plasmids strongly indicates an ultimate bacterial source. It therefore became critical to investigate any potential contaminant in enzymatic or preparative chemical solutions that might yield these sequences, even though gradient fractions with negligible infectivity appeared to be negative for corresponding visible restriction fragments. All control samples, including the many different water samples used, were first subjected to Φ29 polymerase, and then tested by PCR using primers for these two Sphinx sequences. Primers were designed to amplify short regions of the most conserved replicase coding regions. Figure 5 shows a typical PCR example at 18 cycles with a single primer pair alone (e.g., 546 bp for Sphinx 1.76 and 382 bp for Sphinx 2.36) in corresponding lanes 1–5. Neither water, nor Φ×174 DNA that also encodes related replicase proteins, is positive. In contrast, at 18 cycles, the mouse 22L scrapie cells and hamster 263K scrapie-infected brain samples are strongly positive. The FU-CJD-infected mouse brain is similarly positive (data not shown). Furthermore, the parallel gradient sucrose fraction B with lower infectivity also shows a PCR band from Sphinx 1.76 that is less intense than in the more infectious sediment. The less infectious B sucrose fraction contained ~1/20th the amount of fraction A, in reasonable accord with its 50-fold lower infectious titer.

These two primer pairs could be combined to assay for the presence of both Sphinx sequences simultaneously as shown in Fig. 5, lanes 6–9. The PCRs in lanes 6–9 were
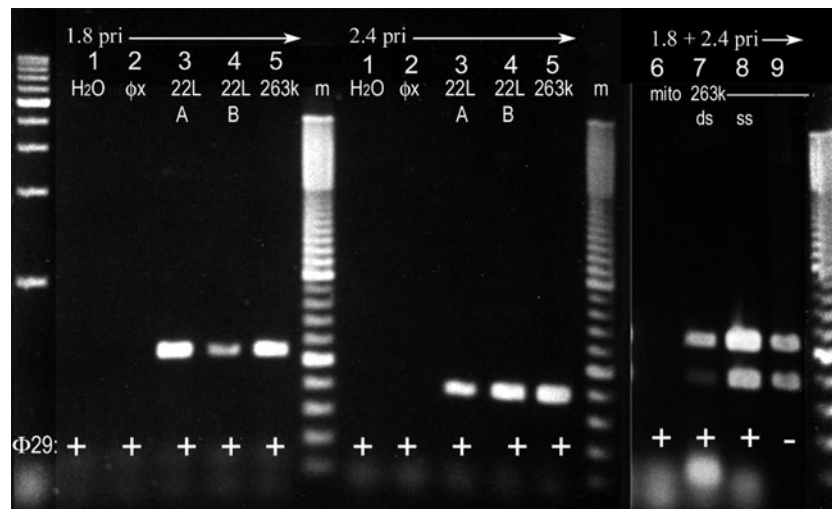

Fig. 5 PCR of Rep coding regions from Sphinx 1.76 and 2.36 separately (*lanes 1–5*, 18 cycles) and together (*lanes 6–9*, 30 cycles). Samples were first synthesized with φ29 polymerase (+ *lanes*) or the initial nucleic acid extract was used for PCR (− *lane*). No bands are seen in the Φ×174 DNA, H₂O, and mitochondrial band even though they all were amplified with φ29 polymerase. There is more Rep 1.8 in the high titer A, versus the lower titer B sucrose gradient fractions; 263K scrapie is from hamster brain. Note ss circular DNA chromatography fraction gives much stronger signals than linear ds DNA fraction (*lanes 7* versus *8*)

subjected to 30 cycles (~1.3 million-fold amplification at 1.6× per cycle determined empirically) to enhance detection of even lower copies. Lane 6 shows the lack of these bands in the PCR product of a control *Xba*I mitochondrial band of ~3.6 kb (see Fig. 3b, lane 2). This mitochondrial band was isolated from an overloaded preparative agarose gel of *Xba*I cut ss DNA and should show a positive signal if the BzNp DEAE medium, agarose or background DNA contained these sequences. In contrast, the enriched circular 263K scrapie hamster brain DNA shows both bands, with a lesser amount of the 1.8kb circle (lower band, lane 7). Moreover, enrichment of DNA circles in the 263K brain fraction using BzNp DEAE demonstrates a much stronger signal of both bands, further confirming their circular nature. The starting DNA extract, before synthesis with Φ29 polymerase, also shows both Sphinx signals. Hence again, as in the water controls, the cytoplasmic particles, not the Φ29 polymerase, are the source of these elements.

Other enzymes and materials that might spuriously contaminate brain and tissue cultures were then systematically tested for these products. PCR for 36–40 cycles after Φ29 polymerase was negative on all of the many independent samples listed in Table 1 (columns 2 and 3). Different sources of enzymes, such as PK, and even 10 mg phenol extracted PK, gave no signal. Infectious preparations made with different detergents and salts also ruled out these materials as the source of Sphinx DNAs. Additionally, these extensive experiments showed that one could have a false negative if samples were not properly purified (see "Materials and methods") or enriched by gradient fractionation. For example, although one total cytoplasmic preparation of control uninfected N2a cultures did not show these bands, the 65% sucrose sediment from this preparation was sufficiently enriched to show a very low yield of these sequences. PCR bands in this sucrose sediment could be visualized at 33 cycles (five million-fold amplification).

Therefore, it was important to test other highly purified normal cell and brain extracts with high PCR cycles to find even trace amounts of these sequences in uninfected preparations that had not shown the characteristic φ29 Sphinx bands. Uninfected hamster brain fractions revealed these bands after 36 cycles of amplification (22 million-fold amplification). These hamster PCR analyses were done without Φ29 polymerase to rule out sample differences that might be skewed by this enzyme. Parallel 263K scrapie-infected hamster samples again contained >2,500-fold amounts of the Sphinx replicase sequences by PCR. Thus, a portion of the replicase domains of both Sphinx sequences were ultimately found in uninfected cells, albeit at much lower level than in infected samples. By PCR, normal material has on average ~1/3,000th the amount found in infected samples. Perhaps this is one of the reasons these sequences have not been previously detected and reported in the database.

Discussion

The current results demonstrate new circular DNAs that concentrate in a variety of highly infectious TSE particle

Table 1 Summary of the number of samples tested for the presence of Sphinx 1.76 and Sphinx 2.36 sequences by PCR of conserved regions (see Fig. 5 examples)

1. Sphinx bands positive by PCR	2. Sphinx bands negative PCR (×40)	3. Additional negatives (×40)
Tissue–cell preparations	Enzymes–biologicals	Buffers, salts, detergents and
22L scrapie: murine N2a cells (*n*=5)	Φ29 polymerase	H$_2$O (*n*=12)
263K scrapie: hamster brain (*n*=3)	RNAse A	Tris buffers (*n*=7)
FU-CJD: mouse brain (*n*=2)	DNAse I	NP-40/DOC (*n*=1)
Uninfected: N2a cells (×33) (*n*=1)	Benzonase	TritonX 100 (n2)
Uninfected hamster brain (×36) (*n*=1)	Roche and BM proteinase K	SDS (*n*=1)
Uninfected mouse brain (×36) (*n*=1)	Phenol extracted 10 mg BM proteinase K	Sarkosyl (*n*=2)
	Φ×174 replicative form	BzNp DEAE (*n*=1)
	Marker DNAs	GdnSCN (*n*=1)
	Agarose	Sucrose (*n*=1)

In positive column 1 samples, *n*=the number of both independent source and preparation. The uninfected cytoplasmic fractions all required ≥33 cycles for visualization, whereas a comparable aliquot of the infectious preparations needed only 13–18 PCR cycles. Comparison of matched parallel normal and infected samples (e.g., normal brain with 263K brain or N2a uninfected cells with 22L scrapie-infected cells, there was a 17–18 cycle difference to obtain a similar band intensity. This represents a >2,500-fold difference in the representation of the replicase region in normal and infected preparations. Enzymes and biologics (column 2) were shown not to be the source of these Sphinx sequences since each enzyme was systematically omitted in different preparations or, where possible, tested by itself with both Φ29 polymerase and maximal PCR cycles (×40). Other sources such as buffers and detergents were also either systematically omitted from different preparations or samples tested directly by Φ29 polymerase followed by 40× cycles of PCR

preparations. TSE samples included monotypic cultures and brain from two species. Three very distinct agent strains (22L scrapie, 263K scrapie, and FU-CJD) were assessed and all were strongly positive for these two Sphinx sequences. Both Sphinx 1.8 and 2.4 kb sequences show a clear viral (plasmid) structure. They are also "functional viruses" because they replicate inside cells and persist after many passages and cell divisions in both N2a and GT cultures. Chromatography, as well as the synthesis of complete mitochondrial DNA circles of 16 kb in sucrose gradient purified samples, further verified the sensitivity, reproducibility, and fidelity of the described preparative, extraction, and ϕ29 polymerase strategy. Whereas past studies of TSE infectious samples have consistently shown only known viral sequences, such as those from endogenous retroviruses, it is clear that unsuspected new sequences with clear viral structures can be identified in infectious TSE agent preparations that have been exhaustively digested with nucleases. Uninfected preparations yielded the same level of mitochondrial DNA bands as TSE-infected preparations. In contrast, high PCR cycles were required to detect the conserved replicase coding regions of the Sphinx sequences in identically processed uninfected cells and brain samples; Sphinx sequences were >2,500-fold greater in infected preparations. Moreover, analysis of sucrose fractions with a significant 50-fold difference in infectious titer showed a corresponding 20-fold difference in the amount of Sphinx 1.76. Hence, these Sphinx sequences copurify and concentrate with infectivity. In addition to conserved viral replicase coding ORFs of 27 and 38 kDa, Sphinx 1.76 DNA has a convincing classical iteron motif for transcriptional function. This function may require appropriate intracellular conditions or host components to participate in infection.

Because Sphinx sequences are present and propagate at very low levels in uninfected cells, it is not yet clear if one or a combination of these sequences can cause infection or carry strain-specific information. Further experiments will also be necessary to determine if there are point mutation(s) that distinguish them from the sequences in normal samples. Other environmental and cell-specific host factors and stresses may also enhance their proliferation and spread, as with other commensal viruses such as the JC papovavirus. Because the Sphinx sequences are already present in rodent cells and brain, one way to assess their role in TSEs would be to target and inhibit these circular DNAs using antisense molecules. If they can be suppressed, and infectivity is significantly reduced or changed, it would be good evidence that they are the long sought informational agent molecules. It will also be of interest to find if these sequences are present in PrP knockout brain. Since PrP is a host molecule required for infection, the presence of Sphinx sequences in knockout mice would not rule out a role for them in infection. However, if Sphinx sequences were absent in PrP knockouts, it would indicate that these circular DNAs require PrP for their persistence.

Nuclei-free cytoplasmic preparations used before sucrose purification (Sun et al. 2008) removed the vast majority of cellular DNA. Direct gel analysis of these more purified cytoplasmic fractions demonstrated removal of all visible RNA after RNAse or Benzonase treatment. Nevertheless, as shown here, complete mitochondrial DNA circles could resist DNAse I and Benzonase under conditions that completely digested naked DNA. Because uninfected cells and brain here lack PrP-res and aggregated PrP amyloid fibrils, neither form was necessary for protection of mitochondrial DNA. Mitochondrial DNA is normally complexed with protein in nucleoids, and this explains their nuclease resistance. Moreover, mitochondrial DNA tenaciously binds PK-insensitive proteins in its D-loop region (Spelbrink 2010; van Tuyle and Pavco 1985). Thus, this DNA region should be preserved in all PK treated scrapie preparations that have been reported to be free of DNA. Indeed, mitochondrial DNA sequences provide a simple internal positive control to show that DNA extractions from infectious cytoplasmic fractions are adequate.

Sphinx circular DNAs can resist nuclease digestion in normal cells that have no PrP-res, indicating Sphinx DNAs are also in a protected or nucleoid form. Indeed, replicase (Rep) proteins bind to iterons, such as the tandem repeats identified in Sphinx 1.76, to establish initiation in the nucleoprotein complex. Hence, Sphinx 1.76 DNA may be similarly protected by its Rep in a protein complex. A mammalian Rep homolog or combined Reps from both Sphinx DNAs might also protect Sphinx 2.36. Moreover, a leucine zipper (LZ) motif, identified in the N-terminal region ORF of Sphinx 1.76, has a conserved structure, and possibly a function that is similar to N-terminal LZ motifs in bacterial Rep plasmids (56); LZ plasmid motifs are responsible for protein dimerization and are involved in DNA binding as well as in conformational protein misfolding. Misfolded PrP-res and amyloid in TSE disease might relate to a similar mechanism. Rep proteins can also be shunted to inaccessible inclusion bodies and require Gdn salts for solubilization (much like PrP-res) when their LZ motif is deleted. These types of observations warrant further investigations of Sphinx functions in TSEs.

In sum, the sequence, structure, and coding capacities of the circular Sphinx DNA elements are viral. They also reside inside the host cell and replicate as do viruses. While their role in infection needs further investigation, so does their potential role in infection-linked tumor formation. A role in tumorigenesis may be

clarified by studies of TSE induced transformed cells (Manuelidis et al. 1987; Manuelidis et al. 1988; Oleszak et al. 1986) as well as with other approaches including high copy transfection. The environmental and homologous sequence connection with selected *A. baumannii* plasmid proteins further suggests that one or more common environmental bacteria, possibly in a symbiotic relationship with mammals, may have transferred at least a part of its protected plasmid DNA to the host. This concept is in keeping with the endosymbiotic origin of mitochondrial DNA from circular genomes of bacteria. Although no trace of bacterial chromosomal DNA has yet been detected in our preparations, *A. baumannii* is a commensal water organism that is commonly found in soil and in association with humans, animals, and insects. It shows a high frequency of antibiotic resistance and infects many people asymptomatically. Nevertheless, it gives rise to many opportunistic hospital infections, including the wounds of soldiers returning from Iraq (Fondi et al. 2010). Because this bacterium is widespread, extensive sensitive combined Φ29 polymerase-PCR tests for Sphinx coding sequences in multiple different water samples and buffers used here (commercial and prepared by four individuals) were analyzed. None were positive. Instead, cells and deep tissues, such as brain, were always required for their detection. The far higher representation of the Sphinx elements in TSE-infected cells and tissues further indicate that these sequences are unlikely to be contaminants of preparative procedures.

The copy number of both Sphinx sequences in infected cells is notably low, and in reasonable accord with 1–20 copies for each infectious TSE agent LD_{50} assayed. This precludes a direct hybridization approach for in-situ detection, especially if their own replicase and/or a host protective protein is impenetrable and prevents access to their DNA in cytologically preserved preparations. However, an alternate approach, one that might also have diagnostic potential, is to make antibodies against the Sphinx Rep proteins using synthetic amino acid sequences for immunization and screening. Finally, it is important to pursue and study other new circular sequences in infectious preparations since one or several of Sphinx elements may act in concert, or depend on one another, to produce infectious disease. There are at least two other new Sphinx elements in infectious fractions that have not yet been systematically tested for their specificity and representation. Additionally, the current agent purification and φ29 polymerase approach can be combined with subtractive strategies, such as representational difference analysis (Dron and Manuelidis 1996), to discover TSE-associated DNAs that are not present in uninfected samples. Many molecules other than PrP remain to be uncovered in TSE infectious fractions, and nucleic acid

sequences related to other circular viruses, such as circoviruses, may be present. Regardless of how Sphinx DNAs ultimately relate to TSE infectivity, tumor formation, and progressive neurodegeneration, the current findings open the door to a more rigorous experimental consideration of a TSE genome. Most intriguing to this writer, given the unexpected finding of persistent plasmid-related elements, is the possibility that mammals may incorporate more of the prokaryotic world in their cytoplasm than previously realized.

Materials and methods

Infectious material Three different sources of infectious material were used. These included the 22L scrapie agent propagated in murine N2a neuroblastoma cells with ~2× 10^8 LD_{50} per gram (equivalent to 10^9 cells) by endpoint titration in mice. This level of infectivity is much higher than found in typical scrapie neuroblastoma cultures (Liu et al. 2008). A rapid 3-week tissue culture infectious dose assay (TCID) with no false background positives (Liu et al. 2008) that is only slightly less sensitive than the 500-day mouse assay, facilitated analysis of the many gradient fractions used here. The purification of infectious particles from 22L scrapie cultures was quantitative, and the sucrose step gradients removed most cellular proteins and 70–80% of PrP and PrP-res as previously depicted (Sun et al. 2008). The bottom 60–65% sucrose gradient fractions with high infectivity by TCID (>5 independent preparations lysed with different detergents) are from those already analyzed and reported in detail (Sun et al. 2008). Hamster brains infected with the 263K scrapie agent (~5×10^9 LD_{50}/g) were homogenized in PBS, and post nuclear supernatants were subjected to comparable sucrose step gradients for infectious particle separation and intracerebral titration in animals. Post-nuclear titered supernatants of mouse brains infected with the Japanese FU-CJD agent were also used for comparison. Several infectious preparations, as well as parallel uninfected controls, were processed both with and without each of the preparative enzymes to rule them out as a contaminating source of circular DNAs. Samples diluted in PBS or TBS prior to nucleic acid extraction were digested with 4 μl RNAase A (Roche) at 37°C for 20–24 h, or with 130 U Benzonase (Sigma) for 2 h at 37°C (supplemented with 2 mM $MgCl_2$); the latter digest was stopped with EDTA pH 8.0 at 5 mM. For DNAse I (Invitrogen) digestion, infectious particles sedimented through detergent free sucrose were diluted in recommended buffer and digested with 200 U for 1 h at 37°C, stopped with EDTA and 0.5% sarkosyl and repurified by sedimentation through a second sucrose step gradient.

Nucleic acid extractions Infectious particles diluted in 50 mM Tris–5 mM EDTA pH 8.0 were first digested with 1 mg/ml proteinase K (PK) for >4 h at 37°C to destroy any endogenous or added nucleases. PK lots were either from Roche or Boehringer Mannheim. SDS or sarkosyl (1%) was then added with a second aliquot of the identical PK and incubated at 37°C for an additional 24 h. After treatment, the mixture had no aggregates and PrP was undetectable on Western blots. The solution was extracted ×3 with phenol: chloroform:isoamyl alcohol (25:24:1) and the aqueous phase re-extracted with chloroform before standard EtOH precipitation using non-biological acrylamide (Ambion) as a carrier. Alternatively, after the initial PK digestion, the preparation was brought to 4 M GdnSCN pH 7 (Fluka) and heated at 55°C for 1–2 h. It was then diluted to 1 M GdnSCN and digested with fresh PK for >2 h before either EtOH precipitation or purification on a Machery Nagel Nucleospin II column per manufacturer's instructions. Both nuclease digestions were monitored by nanodrop and gel analysis, and both markedly reduced RNA by ≥1,000-fold, with only a small residue of material at <50 nt.

Φ29 polymerase and ssDNA chromatography In general, nucleic acids extracted from material with a total of ~5× 10^6 LD_{50} were mixed in a 10 μl reaction that included 25 μM Φ29 random hexamer primers with 3′ thiophosphate protected ends (Fidelity Systems), 600 μM each dNTPs, and 0.3 μl (3.3 u) of Φ29 polymerase (NE Biolabs) in their supplied buffer supplemented with 1 μg/μl BSA. The mixture was incubated for 12–13 h at 30°C (found to be optimal for high yields) and 1% agarose TAE gels were loaded with 0.5 μl of the reaction. Heating of samples, required to denature ds DNA, did not result in different bands or a greater yield, and was omitted. When infectious preparations were not pretreated with RNAse prior to extraction there were microgram amounts of a smear of RNA up to 10 kb from preparations with ~10^7 TCID. For Φ29 polymerase, these RNAs were inhibitory and had to be removed by RNAse digestion followed by Nucleospin column purification, probably because they annealed to the random primers. Notably, DNA synthesis was also completely inhibited by RNAse, as well as by trace phenol and other impurities. For enrichment of circular ss DNAs, extracted nucleic acids were separated on Clontech SSAM PCR purification kit per instructions. Washed Benzoylated Napthoylated DEAE Cellulose (BZNp DEAE, Sigma) was also used identically with the sample applied in 0.3 M NaCl in TE. The linear dsDNA was eluted with 1 M NaCl in TE, and the ss and circular DNAs eluted with 1 M NaCl–TE with 2% caffeine. Controls showed that a mix of circular Φ×174 RF circles and linear DNA size markers were separated (Fig. 3). Eluted samples were precipitated with EtOH and solubilized in a small volume of 5 mM Tris–Cl pH 8.0. These columns were also useful for removing primers and ssDNA from PCR reactions.

Restriction enzyme analysis, PCR and sequencing Restriction enzymes from NE Biolabs were used to digest Φ29 polymerase products. For amplification of fragments of interest, DNA bands were cut from gels, purified on Nucleospin columns, and ligated to 24/12 primers appropriate for the 5′ overhang ends. For *Eco*RI and *Xba*I cut circles, the "6F4" ligation sequence: 5′ CCAAG ATGCTCGAGGTGTACGCCC was annealed to either 5′ AATTGGGCGTACAC for EcoRI, or 5′ CTAGGGG CGTACAC for *Xba*I. RBgl and NBgl 24/12 ligators as previously described (Dron and Manuelidis 1996) were also mixed 1:1 for the ligation reaction to the *Bgl*II restriction fragment. The eluted DNA band was mixed with 15 μM of each ligator primer in 1× T4 ligase buffer (GibcoBRL), heated to 50°C for 1 min and cooled at 0.8°C/min to10°C; 1 μl T4 ligase (400 U, NE Biolabs) was then added for incubation at 13°C for 16 h. The sample was diluted and used for fill-in (28″ at 68°C and 10 min at 70°C) with subsequent PCR in 50 μl reactions with the 24mers 6F4 or Bgl primers, dNTPs, and Elongase (GibcoBRL) in the recommended conditions. Elongase yielded the largest PCR products. This included copurifying mitochondrial DNA restriction fragments of ~10 kb that were partially sequenced in parallel to Sphinx bands as internal controls. For initial sequencing, PCR bands were cut with an appropriate restriction enzyme (e.g., see Fig. 2, lane 8), and the 3′ and 5′ end fragments were separated on agarose gels, stained with Sybr Gold, eluted, and mixed with appropriate 24mer ligators for sequencing. From obtained initial sequences, internal primers for PCR walks were designed and yielded overlapping sequence confirmation of the complete circle. Automated sequencing was done by the Yale Keck facility.

References

Aiken JM, Williamson JL, Marsh RF (1989) Evidence of mitochondrial involvement in scrapie infection. J Virol 63:1686–1694

Aiken JM, Williamson JL, Borchardt M, Marsh RF (1990) Presence of mitochondrial D-loop DNA in scrapie-infected brain preparations enriched for prion protein. J Virol 64:3265–3268

Akowitz A, Sklaviadis T, Manuelidis L (1994) Endogenous viral complexes with long RNA cosediment with the agent of Creutzfeldt–Jakob disease. Nucleic Acids Res 22:1101–1107

Alais S, Simoes S, Baas D, Lehmann S, Raposo G, Darlix J, Leblanc P (2008) Mouse neuroblastoma cells release prion

infectivity associated with exosomal vesicles. Biol Cell 100:603–615

Arjona A, Simarro L, Islinger F, Nishida N, Manuelidis L (2004) Two Creutzfeldt–Jakob disease agents reproduce prion protein-independent identities in cell cultures. Proc Natl Acad Sci USA 101:8768–8773

Baker CA, Martin D, Manuelidis L (2002) Microglia from CJD brain are infectious and show specific mRNA activation profiles. J Virol 76:10905–10913

Bian J, Napier D, Khaychuck V, Angers R, Graham C, Telling G (2010) Cell-based quantification of chronic wasting disease prions. J Virol 84:8322–8326

Bruce ME, Dickinson AG (1987) Biological evidence that scrapie has an independent genome. J Gen Virol 68:79–89

Couzin-Frankel J (2010) Prion diseases: no accomplice needed. Science-NOW. Available at http://news.sciencemag.org/sciencenow/2010/01/28-03.html

Davidson I, Shulman L (2008) Unraveling the puzzle of human anellovirus infections by comparison with avian infections with the chicken anemia virus. Virus Res 137:1–15

Dean F, Nelson J, Giesler T, Lasken R (2001) Rapid amplification of plasmid and phage DNA using Phi 29 DNA polymerase and multiply-primed rolling circle amplification. Genome Res 11:1095–1099

Diringer H, Gelderblom H, Hilmert H, Ozel M, Edelbluth C, Kimberlin RH (1983) Scrapie infectivity, fibrils and low molecular weight protein. Nature 306:476–478

Dron M, Manuelidis L (1996) Visualization of viral candidate cDNAs in infectious brain fractions from Creutzfeldt–Jakob disease by representational difference analysis. J Neurovirol 2:240–248

Edgeworth J, Gros N, Alden J, Joiner S, Wadsworth J, Linehan J, Brandner S, Jackson G, Weissmann C, Collinge J (2010) Spontaneous generation of mammalian prions. Proc Natl Acad Sci USA 107:14402–14406

Elsner C, Dörries K (1992) Evidence of human polyomavirus BK and JC infection in normal brain tissue. Virology 191:72–80

Falsig J, Nilsson K, Knowles T, Aguzzi A (2008) Chemical and biophysical insights into the propagation of prion strains. HFSP J 2:332–341

Fondi M, Bacci G, Brilli M, Papaleo M, Mengoni A, Vaneechoutte M, Dijkshoorn L, Fani R (2010) Exploring the evolutionary dynamics of plasmids: the Acinetobacter pan-plasmidome. BMC Evolutionary Biol 10:59

Franklin R (1956) X-ray diffraction studies of cucumber virus and three strains of tobacco mosaic virus. Biochim et Biophys Acta 19:203–211

Geoghegan J, Valdes P, Orem N, Deleault N, Williamson R, Harris B, Supattapone S (2007) Selective incorporation of polyanionic molecules into hamster prions. J Biol Chem 282:36341–36353

Kekarainen T, Martínez-Guinó L, Segalés J (2009) Swine torque teno virus detection in pig commercial vaccines, enzymes for laboratory use and human drugs containing components of porcine origin. J Gen Virol 90:648–653

Li J, Browning S, Mahal S, Oelschlegel A, Weissmann C (2010) Darwinian evolution of prions in cell culture. Science 327:869–872

Liu Y, Sun R, Chakrabarty T, Manuelidis L (2008) A rapid accurate culture assay for infectivity in transmissible encephalopathies. J NeuroVirol 14:352–361

Ma S, Sakugawa H, Makino Y, Tadano M, Kinjo F, Saito A (2003) The complete genomic sequence of hepatitis delta virus genotype IIb prevalent in Okinawa, Japan. J Gen Virol 84:461–464

Maggi F, Fornai C, Vatteroni M, Siciliano G, Menichetti F, Tascini C, Specter S, Pistello M, Bendinelli M (2001) Low prevalence of TT

virus in the cerebrospinal fluid of viremic patients with central nervous system disorders. J Med Virol 65:418–422

Manuelidis L (1994) Dementias, neurodegeneration, and viral mechanisms of disease from the perspective of human transmissible encephalopathies. Ann NY Acad Sci 724:259–281

Manuelidis L (1997) Beneath the emperor's clothes: the body of data in scrapie and CJD. Annales de L'Institute Pasteur 8:311–326

Manuelidis L (2003) Transmissible encephalopathies: speculations and realities. Viral Immunology 16:123–139

Manuelidis L (2007) A 25 nm virion is the likely cause of transmissible spongiform encephalopathies. J Cell Biochem 100:897–915

Manuelidis L (2010) Transmissible encephalopathy agents: virulence, geography and clockwork. Virulence 1(2):101–104

Manuelidis L, Manuelidis EE (1981) Search for specific DNAs in Creutzfeldt–Jakob infectious brain fractions using nick translation. Virol 109:435–443

Manuelidis L, Ward DC (1984) Chromosomal and nuclear distribution of the Hind III 1.9 kb repeat segment. Chromosoma (Berl) 91:28–38

Manuelidis E, Fritch W, Kim J, Manuelidis L (1987) Immortality of cell cultures derived from brains of mice and hamsters infected with Creutzfeldt–Jakob disease agent. Proc Natl Acad Sci 84:871–875

Manuelidis L, Murdoch G, Manuelidis E (1988) Potential involvement of retroviral elements in human dementias. Ciba Found Symp 135:117–134

Manuelidis L, Sklaviadis T, Akowitz A, Fritch W (1995) Viral particles are required for infection in neurodegenerative Creutzfeldt–Jakob disease. Proc Natl Acad Sci USA 92:5124–5128

Manuelidis L, Yu Z-X, Barquero N, Mullins B (2007) Cells infected with scrapie and Creutzfeldt–Jakob disease agents produce intracellular 25-nm virus-like particles. Proc Natl Acad Sci USA 104:1965–1970

Manuelidis L, Chakrabarty T, Miyazawa K, Nduom N-A, Emmerling K (2009a) The kuru infectious agent is a unique geographic isolate distinct from Creutzfeldt–Jakob disease and scrapie agents. Proc Natl Acad Sci USA 106:13529–13534

Manuelidis L, Liu Y, Mullins B (2009b) Strain-specific viral properties of variant Creutzfeldt–Jakob Disease (vCJD) are encoded by the agent and not by host prion protein. J Cell Biochem 106:220–231

Merz PA, Somerville RA, Wisniewski HM, Manuelidis L, Manuelidis EE (1983) Scrapie associated fibrils in Creutzfeldt–Jakob disease. Nature 306:474–476

Mizuta R, Mizuta M, Kitamura D (2003) Atomic force microscopy analysis of rolling circle amplification of plasmid DNA. Arch Histol Cytol 66:175–181

Miyazawa K, Emmerling K, Manuelidis L (2010) Proliferative arrest of neural cells induces prion protein synthesis, nanotube formation, and cell-to-cell contacts. J Cell Biochem 111:239–247

Navidad P, Li H, Mankertz A, Meehan B (2008) Rolling-circle amplification for the detection of active porcine circovirus type 2 DNA replication in vitro. J Virol Methods 152:112–116

Nicoll A, Collinge J (2009) Preventing prion pathogenicity by targeting the cellular prion protein. Infect Disord Drug Targets 9:48–57

Nishida N, Katamine S, Manuelidis L (2005) Reciprocal interference between specific CJD and scrapie agents in neural cell cultures. Science 310:493–496

Oesch B, Groth DF, Prusiner SB, Weissmann C (1988) Search for a scrapie-specific nucleic acid: a progress report. Ciba Found Symp 135:209–217

Oleszak E, Manuelidis L, Manuelidis EE (1986) In vitro transformation elicited by Creutzfeldt–Jakob infected brain material. J Neuropathol Exp Neurol 45:489–502

Prusiner SB (1982) Novel proteinaceous infectious particles cause scrapie. Science 216:136–144

Prusiner S, Baldwin M, Collinge J, DeArmond S, Marsh R, Tateishi J, Weissmann C (1995) Prions. Springer, Wien

Safar J, Kellings K, Serban A, Groth D, Cleaver J, Prusiner S, Riesner D (2005) Search for a prion-specific nucleic acid. J Virol 79:10796–10806

Shlomchik M, Radebold K, Duclos N, Manuelidis L (2001) Neuroinvasion by a Creutzfeldt–Jakob disease agent in the absence of B cells and follicular dendritic cells. Proc Natl Acad Sci USA 98:9289–9294

Sklaviadis T, Dreyer R, Manuelidis L (1992) Analysis of Creutzfeldt–Jakob disease infectious fractions by gel permeation chromatography and sedimentation field flow fractionation. Virus Res 26:241–254

Spelbrink J (2010) Functional organization of mammalian mitochondrial DNA in nucleoids: history, recent developments, and future challenges. IUBMB Life 62:19–32

Sun R, Liu Y, Zhang H, Manuelidis L (2008) Quantitative recovery of scrapie agent with minimal protein from highly infectious cultures. Viral Immunol 21:293–302

Supattapone S (2010) Biochemistry. What makes a prion infectious? Science 327:1091–1092

Taruscio D, Manuelidis L (1991) Integration site preferences of endogenous retroviruses. Chromosoma 101:141–156

van Tuyle G, Pavco P (1985) The rat liver mitochondrial DNA–protein complex: displaced single strands of replicative intermediates are protein coated. J Cell Biol 100:251–257

Vincent I, Carrasco C, Guzylack-Piriou L, Herrmann B, McNeilly F, Allan G, Summerfield A, McCullough K (2005) Subset-dependent modulation of dendritic cell activity by circovirus type 2. Immunology 115:388–398

Zou W, Gambetti P (2007) Prion: the chameleon protein. Cell Mol Life Sci 64:3266–3270